

AD-A162 035

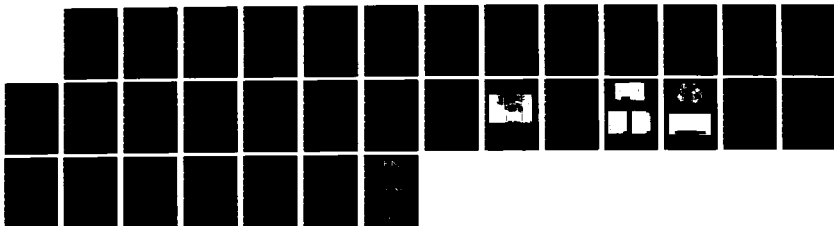
A FUNDAMENTAL STUDY OF DROPLET IMPINGEMENT SPREADING  
AND CONSOLIDATION(U) DREXEL UNIV PHILADELPHIA PA DEPT  
OF MATERIALS ENGINEERING D APELIAN ET AL 01 SEP 85  
TR-1 N00014-84-K-0472

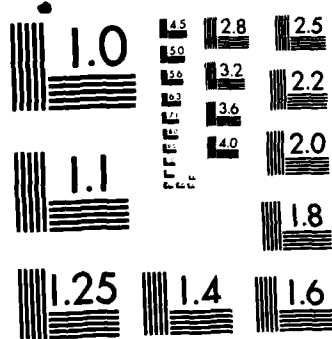
1/1

UNCLASSIFIED

F/G 7/1

NL





MICROCOPY RESOLUTION TEST CHART  
NATIONAL BUREAU OF STANDARDS-1963-A

12

Technical Report No. 1

Contract N 00014-84-K-0472; NR 650-025

## AD-A162 035

### A FUNDAMENTAL STUDY OF DROPLET IMPINGEMENT, SPREADING AND CONSOLIDATION

D. Apelian, A. Lawley, G. Gillen and P. Mathur  
Department of Materials Engineering  
Drexel University  
Philadelphia, PA 19104

1 September 1985

Annual Report for Period 1 July 1984 - 30 June 1985

Approved for public release; distribution unlimited. Reproduction in whole or in part is permitted for any purpose of the United States government.

Prepared for  
OFFICE OF NAVAL RESEARCH  
800 N. Quincy Street  
Arlington VA 22217

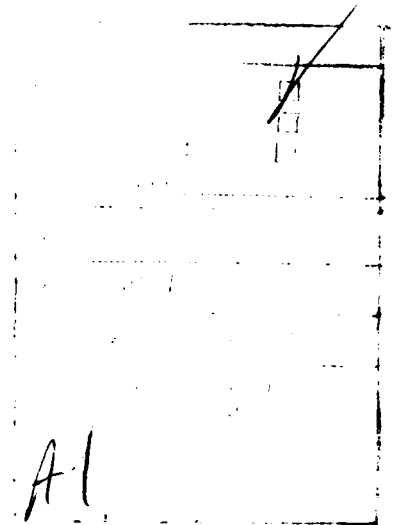


DTIC FILE COPY

85 11 26 007

## TABLE OF CONTENTS

ABSTRACT	i
INTRODUCTION	1
DREXEL'S SPRAY FORMING FACILITY	2
(a) Melting System	3
(b) Nitrogen Gas Atomization Process	3
(c) Substrate Configuration and Movement	4
RESEARCH PROGRAM	4
(a) Experimental Studies	4
The Melt	5
Atomization	6
Metal Spray	7
Substrate	7
Results	8
(b) Modeling Studies	9
Droplet Velocity	10
Droplet Temperature	12
Droplet Consolidation	14
(c) Future Research	15
Short Term Objectives	15
Long Term Objectives	16
REFERENCES	
FIGURES	
APPENDIX I	
APPENDIX II	



## ABSTRACT

Spray forming in the Osprey mode is a process in which gas atomized molten metal droplets are interrupted in flight by impingement on a substrate to form a relatively thick deposit. The overall objective of this research program is to develop a fundamental processing science base for the process. To this end, concurrent experimental and modeling studies focus on droplet velocity and temperature profiles, the mechanism(s) of droplet-substrate interactions, droplet spreading on impact and droplet solidification, and the relationship between process parameters and microstructural integrity of the deposit. On-going experimental studies are reviewed and some preliminary results of the modeling work are presented.

## INTRODUCTION

Spray forming is the generic name given to a new generation of net or near net shape processes in which a stream of molten metal droplets is interrupted in flight by impingement on a substrate. The droplets are molten or partially solidified on impact with the substrate and subsequently spread, flatten, and coalesce to form a thick, coherent deposit.

There are several advantages of spray forming compared to ingot or powder metallurgy processes. Firstly, spray forming provides a direct route from the molten metal to a near-net preform or net shape with significant cost savings compared to ingot casting. Secondly, solidification of the impinging droplets occurs under conditions of rapid solidification, with attendant fine grain size, the absence of macrosegregation and improved workability in the final product. Thirdly, the benefits of powder metallurgy can be achieved without the problems associated with the storing and handling of powders.

There are several modes of spray forming. In spray rolling, a continuous strip is deposited, followed by hot or cold rolling. Spray forging involves the spray casting of a preform which is subsequently hot forged to final shape. When the spray deposit is in the form of a thin coating on the substrate, the process is termed spray coating. In centrifugal spray deposition, the molten metal is centrifugally atomized and deposited on to a surrounding circular substrate. Spray forming has also been used to produce laminated products by means of two or more independent spray sources. By introducing ceramic particles into the spray of molten droplets it is possible to fabricate composite materials.

The stream or spray of molten droplets can be generated by the gas atomization of molten metal, or by feeding the alloy, in the form of powder or wire, into a plasma or laser beam. The corresponding spray forming technologies are known as the Osprey process, low pressure plasma deposition, and layerglazing, respectively. The present program constitutes a basic study of the Osprey process. Technologically, this

approach is attractive since the rate of deposition is high, of the order of 1 kg/s.

### PROGRAM OBJECTIVES

The overall objective of this research program is to establish a fundamental processing science base for spray forming in the Osprey mode. In particular, what are the mechanisms of consolidation of molten or partially molten particles impinging on a substrate? To this end, spray forming experiments, carried out in a new in-house Osprey unit, are directed to droplet-substrate interactions, droplet spreading on impact, and droplet solidification. Concurrent modeling studies are designed to predict droplet spreading and consolidation behavior on impact with the substrate. Primary outputs of the modeling phase of the program are droplet velocity and temperature profiles, and droplet shape as a function of time as the droplet contacts the substrate.

### DREXEL'S SPRAY FORMING FACILITY

Drexel's spray forming unit is shown in Figure 1. Major components of the equipment and the process can be described in terms of: (i) the melting system, (ii) the nitrogen gas atomization process and (iii) the configuration and movement of the substrate. The deposition process is shown schematically in Figure 2. A detailed chronology of the acquisition, installation, commissioning and operation of the unit is given in Appendix I.

### (a) Melting System

The material to be spray deposited is placed in an alumina crucible which can hold up to 30 kg of metal. A surrounding protective cage keeps the crucible wall under compression and arrests the flow of molten metal in the event of a break-out. The protective cage consists of a sand-based ramming mix confined within a thin-walled cylinder of stainless steel. The protective cage, crucible and charge are placed inside the induction coil box which sits on the atomizing block at the top of the spray chamber. An Inductotherm 180kW induction generator supplies power to the coil box.

During melting the chamber is purged with nitrogen gas and a slight overpressure of nitrogen gas is fed into the sealed crucible to prevent the material from oxidizing. The melting system is designed so that metal at the bottom of the crucible is the last to melt. When this melts all of the molten metal starts to pour through a refractory zirconia nozzle in the bottom of the crucible. A stream of molten metal, the diameter of which is the same as the diameter of the refractory nozzle, then pours into the atomizing zone.

### (b) Nitrogen Gas Atomization Process

In the atomizing region the molten metal stream is broken-up into a spray of small droplets by a high pressure of nitrogen gas. An Airco storage vessel, which can hold up to 70 inches water gage pressure of liquid nitrogen, supplies the atomizing gas. It is connected to a large vaporizer which provides a high volume flow of the atomizing gas when required. The flow of nitrogen into the atomizer block is regulated by a gas control panel specially designed for Drexel's plant. Typically, the atomizing gas pressure is 120psi but up to 220psi can be supplied to the spray forming equipment. The flow rate of molten metal into the atomizing region is determined by the diameter of the stream and the head of metal in the crucible. The nitrogen gas overpressure to the top of the crucible is used to compensate for the falling head of metal. The overpressure can also be varied slightly to change the metal flow rate as required.



### (c) Substrate Configuration and Movement

The molten droplets are cooled and accelerated towards the substrate by the atomizing gas. The temperature and velocity of the droplets in the metal spray determine how they will spread and solidify on impact with the substrate. The substrate can be traversed in a direction normal to the axis of the metal spray. It can also be rotated at the same time. Depending on the size and configuration of the substrate, preforms of various shapes can be produced. A solid circular preform can be manufactured by using a rotating disc as a substrate. A rotating mandrel can be coated with a thin layer of spray deposited material. Alternatively, a thick walled deposit can be allowed to build up over a period of time. Flat substrates can also be used to obtain a fundamental understanding of the spray forming process.

An optical pyrometer which is positioned on top of the spray chamber is focused on the substrate to record the temperature of the deposit. The pyrometer is also connected to a microprocessor in the gas control panel. If the temperature of the deposit is higher than a pre-set value, the microprocessor will increase the atomizing gas pressure thus reducing the temperature of the metal spray. Alternatively, the metal flow rate can be reduced by decreasing the overpressure to the top of the crucible.

## RESEARCH PROGRAM

### (a) Experimental Studies

The main objective of the research is to identify and understand the mechanisms of droplet consolidation. The initial phase of research involves a fundamental study of spray deposition onto flat substrates. In particular, those spray forming parameters which influence the atomization and deposition processes will be identified. In spray forming

it is convenient to consider processing and material parameters in four categories :

- (i) melt system
- (ii) atomization
- (iii) metal spray
- (iv) substrate

Each of the above components of the spray forming process is now considered with respect to the ongoing research program.

### The Melt

Major variables are alloy composition, charge and melt preparation, melt superheat and melt overpressure. A matrix of experiments is being conducted to determine which parameters are the most influential in the deposition and consolidation processes. Specific alloy systems have been selected for examination on the basis of known relationships between spray forming process parameters and microstructure. The microstructure of tool steels is known to be particularly sensitive to changes in the process parameters. Carbide compositions vary significantly with spray forming conditions. M2 tool steel is being used for the initial study of the deposition process.

In addition to tool steels other alloy systems will be investigated. A number of alloys in the Ni-Cr system will be sprayed. This will delineate variations in consolidation behaviour with freezing range and composition. In particular, the following systems will be evaluated :

pure Ni	melting point: 1455 °C
Ni-20wt.% Cr	freezing range: 20 °C

Ni-51wt.% Cr	eutectic composition
Ni-70wt.% Cr	freezing range 250 °C
(Ni-Al) - Cr	quasi-binary eutectic

The Fe-Mn and Fe-Cu systems exhibit a large difference in freezing range for the same liquidus temperature and solute content :

Fe-20wt.% Mn	$T_L = 1450\text{ °C}$ ; freezing range = 20 °C
Fe-20wt.% Cu	$T_L = 1450\text{ °C}$ ; freezing range = 350 °C

In the Fe-B-Si system a crystalline structure is obtained when the material is quenched at a cooling rate less than  $10^5\text{ K/s}$ , and an amorphous structure above  $10^5\text{ K/s}$ . The scale of the crystalline microstructure will provide an estimate of cooling rates below  $10^5\text{ K/s}$ .

The gas overpressure will be varied to provide a range of values of the metal : gas mass flow rates. Superheat will be varied in order to assess the effect of melt viscosity and surface tension on the resulting spray deposit.

### Atomization

The ratio of the metal to gas mass flow rates is a critical parameter in the atomization and deposition processes. An increase in the flow rate of molten metal is brought about by enlarging the diameter of the refractory nozzle or by increasing the nitrogen gas overpressure to the top of the crucible. An increase in the gas flow rate can be achieved by increasing the supply pressure. A second atomizer block which has larger diameter nozzles for the nitrogen gas can also be utilized. These

process parameters will be controlled and varied systematically.

### Metal Spray

Both the density of the spray (no. of droplets/sec./area) and the uniformity of the spray are key factors in relation to the deposit integrity. Spray density is primarily a function of the ratio of metal to gas mass flow rates. In addition to spray density, this ratio also influences the average droplet diameter and droplet size distribution. To optimize the spray process, the temperature and velocity of the droplets must be known throughout the melt spray region and on impact with the substrate. Both of these droplet properties are affected primarily by the velocity and temperature of the surrounding nitrogen gas. The gas cools the molten droplets by forced convection. Experimentally, high speed video cameras will be utilized to characterize the spray zone in Figure 2. A qualitative indication of the spray temperature is afforded by color photography. In addition, computer modeling will be used to calculate velocity and temperature profiles of the metal droplets and predict their subsequent splatting and solidification behavior.

### Substrate

Initially deposition onto flat substrates is being carried out. This will provide a fundamental understanding of droplet consolidation with increase in deposit thickness. Both an insulating refractory material and a high conductivity metal are being used as substrates. Thermocouples will be embedded in the substrate and the deposit to measure temperature and monitor heat flow. The changes in heat flow conditions with variations in the thermal characteristics of the substrate material will be studied.

## Results

Run 1 : A solid disc shaped preform of M2 tool steel was spray deposited as part of the commissioning between Drexel and Osprey. A listing of the operating conditions is given in Appendix II. The gas atomization pressure was set at 100psi. This pressure was not high enough to cool the metal droplets adequately. As a result the deposit temperature was too hot and the preform contained macroporosity. The preform was sectioned and examined on the optical microscope showing a uniform homogeneous microstructure of fine-scale martensite interspersed with  $M_6C$  carbides. The video showed the build-up of the deposit but no individual droplets were observed at the slowest play-back speed of 1 frame per 1/30 second. However at this play-back speed the spray density was seen to vary from frame to frame. This may be the result of the formation and break-up of the "cone" at the bottom of the metal stream during atomization. Similar "cone" formation during atomization has been observed by other researchers.

Run 2 : It was decided that the first run carried out solely by the Drexel research team should also be a solid disc preform of M2. This is shown in Figure 3. The gas atomization pressure was increased to 116psi but no other parameters were changed. The macroporosity level was reduced considerably. The preform was sectioned and examined in the SEM. A typical martensite plus carbide microstructure is shown in Figure 4. In the region nearest to the substrate the structure was much finer as shown in Figure 5. Isolated eutectic areas, indicative of regions of slow cooling or trapped liquid, were also visible as shown in Figure 6.

During this run the video was set up to view the atomization process. Unfortunately it was focused just below the point of atomization and only the spray was visible and not the metal stream. Once again the spray density was seen to vary at slow play-back speeds. For a few seconds at the start of the run the gas atomization pressure was 87psi before it increased to 116 psi for the rest of the run. When the increase occurred the spray became slightly wider and the atomization point

appeared to move closer to the atomization block.

Run 3 : M2 was deposited under atomization conditions similar to Run 2 onto two long flat substrates placed side by side. One substrate was copper and the other was an alumina-based refractory. The substrates were positioned either side of the center of the spray axis. The run lasted approximately 40 seconds:

- (i) For 20 secs both substrates were oscillated back and forth beneath the spray. This allowed a multi-pass deposit to build-up.
- (ii) For the remaining 20 secs an unsprayed substrate was placed beneath the spray and kept stationary until the end of the run.

The resultant shapes from the two modes are shown in Figure 7. With the substrate stationary, the outside of the deposit exhibits a "feathery" morphology - left side of Figure 7. The "feathers" begin as small perturbations near the base of the deposit and grow outwards as the size of the preform increases rapidly upwards. The deposit has been sectioned in preparation for metallographic examination.

In subsequent runs, a thermocouple will be used to measure the melt temperature. Thermocouples will also be embedded in the substrate and deposit. They will interface with a computer to record temperature, and to monitor changing conditions of heat flow.

#### (b) Modeling Studies

The role of modeling in this study is to predict the spreading and consolidation behavior of droplets on impact with the substrate. The integral model is divided into two parts: the velocity and temperature profiles of the droplets in flight, and the subsequent splatting and consolidation on the substrate.

### Droplet Velocity

In formulating the model for predicting the velocity and temperature dependence of droplets as a function of flight distance, the following assumptions have been made:

(i) Each droplet is treated as a rigid sphere of diameter  $d$ . Although the droplets are initially ligament-shaped, the time for spherodization [1] is of the order of  $10^{-7}$  seconds. This is much shorter than the flight time of a few milliseconds predicted by the model.

(ii) Droplets of equal size travel with the same velocity and follow a linear trajectory. Since there are droplets of varying sizes travelling at different speeds in a small volume there is a definite possibility of droplet collisions and/or coalescence. However, no calculations on the probability of such events is being attempted in the initial modeling studies.

(iii) The flight distance is measured from the point of atomization.

Each droplet formed from the "atomization cone" [2] is accelerated towards the substrate by the high velocity atomizing gas jets and, to a lesser extent, by the gravitational force acting on it. The total force acting on the droplet is given by [3]:

$$F = Ma = 0.5 C_D \rho_g V_r^2 S + Mg \quad \dots (1)$$

where,

- $M$  = mass of the droplet
- $a$  = acceleration =  $dV_d/dt$
- $C_D$  = drag coefficient
- $\rho_g$  = density of the gas
- $V_r$  = droplet velocity ( $V_d$ ) relative to the gas
- $S$  = droplet cross-sectional area
- $g$  = acceleration due to gravity

Although several other relationships have been proposed to predict the velocity profile of droplets in a gas stream [4,5,6], good agreement is reported [1,7] between photographic measurements and predictions based on equation (1). The earlier work [1] was, however, carried out on water droplets which shattered after a few inches of flight and further correlation was impossible.

There is no analytical solution to equation (1), and it can only be solved numerically at nodes positioned infinitesimally apart along the trajectory of the droplet. The velocity of the metal stream at the point of atomization is of the order of 2-8 m/s. In the model, the initial velocity of the droplet at the point of atomization is assumed to be zero based on measurements of Naida et. al. [1] for the atomization of bronze. A sensitivity analysis was carried out to determine the effect of varying initial velocity on the subsequent velocity profile of the droplet. In the range 0-10 m/s, initial droplet velocity does not appear to have a significant effect on the subsequent velocity profile of the droplet.

Many empirical and semi-empirical relationships have been proposed to approximate the standard drag on a spherical body moving in a steady viscous flow. The drag coefficient ( $C_D$ ) proposed by Kurten et. al [8] was adopted since it is applicable for a wide range of Reynolds numbers (0.1-4000), with a small deviation ( $\pm 7\%$ ) from the standard drag curve.

$$C_D = 0.28 + 6/\sqrt{Re} + 21/Re \quad \dots (2)$$

$$Re = V_r d \rho_g / \mu_g$$

where  $Re$  is the Reynolds number,  $d$  the diameter of the droplet and  $\mu_g$  the gas viscosity. Lesinski et. al. [9] used a series of expressions for the drag coefficient to approximate the standard drag curve over a large range of Reynolds numbers. There appears to be appreciable correlation between their model and the measurements of gas/droplet velocity by Laser Doppler Anemometry. Therefore the drag coefficients proposed by them have also been tried.



### Droplet Temperature

Newtonian cooling conditions (Biot number,  $Bi > 2$ ) are usually assumed to apply to gas atomization and the heat transfer is expected to be interface controlled rather than by the thermal properties of the metal. Under these conditions the droplet temperature remains nearly uniform in the liquid during cooling and solidification, if this occurs at sufficiently low undercooling. The convective heat transfer is estimated from the following well established empirical equation by Ranz and Marshall [10]:

$$Nu = hd/k_g = 2.0 + 0.6 Re^{0.5} Pr^{0.33} \quad \dots (3)$$

where  $Nu$  = Nusselt number  
 $d$  = droplet diameter  
 $h$  = heat transfer coefficient  
 $k_g$  = thermal conductivity of the gas  
 $Pr$  = Prandtl number ( $= c_g \mu_g / k_g$ )  
 $c_g$  = specific heat of the gas

$Re$  is calculated from the model for droplet velocity. The heat transfer coefficient is then computed using equation 3 and a correction factor to take into account the temperature of gas immediately neighbouring the droplet [11]. Assuming complete temperature uniformity in the interior of the droplet, the heat balance is given by:

$$\begin{aligned} \text{heat lost by droplet} &= \text{heat loss by forced convection} + \text{radiative heat loss} \\ &= h A (T_d - T_g) dt + \sigma \epsilon A (T_d^4 - T_g^4) dt \quad \dots (4) \\ &= \text{heat gained by atomizing gas} \end{aligned}$$

where  $A$  = surface area of the droplet  
 $T_d$  = instantaneous droplet temperature  
 $T_g$  = average gas temperature  
 $dt$  = time for droplet to travel between two successive nodes  
 $\sigma$  = stefan-boltzman constant  
 $\epsilon$  = emissivity of the droplet

The change in temperature of the droplet between two successive nodes is given by:

$$\Delta T_d = (\text{total heat lost}) / c_p \quad \dots (5)$$

The rise in temperature of the gas is calculated similarly by taking into account the ratio of metal to gas mass flow rates. Variation of the thermal properties of both gas and metal with temperature have also been incorporated in the model.

Figure 8 shows the variation of the gas and droplet velocities with flight distance for aluminum alloy droplets. Computer simulation predicts that the velocity of a 20 $\mu\text{m}$  droplet reaches a maximum of ~150 m/s at a distance of 100 mm from the point of atomization, while a 50 $\mu\text{m}$  droplet is accelerated to ~100 m/s nearly 200 mm away. The expression for the drag coefficient by Lesinski, et. al [9] predicts a steeper rise in droplet velocity than the expression for  $C_D$  by Kurten, et. al. [8]; as shown in Figure 8(b).

Figure 9 depicts the variation of relative velocity and droplet acceleration with flight distance. The relative velocity is a maximum at the point of atomization and is the accelerating force on the droplet in flight. Therefore the acceleration of the droplet decreases sharply with decreasing relative velocity, reaches a minimum, and then slowly increases corresponding to a rise in relative velocity. The temperature profiles of two droplets, 20 $\mu\text{m}$  and 50 $\mu\text{m}$  in diameter, are shown in Figure 10. Relative velocity is also the most significant factor responsible for droplet cooling. Correspondingly, the cooling of the droplets is rapid in the initial stages of flight and then gets retarded. However, there is an abrupt increase in cooling rate at the end of the freezing range (Figure 11). The degree of superheat appears to have a negligible effect on the velocity of the droplet, but a marked effect on its temperature profile, as shown in figure 12.

The results from the model will subsequently be confirmed by experimental measurement of important variables such as the gas velocity profile, droplet temperature, temperature of the exhaust gases, etc.

### Droplet Consolidation

Modeling of the droplets contacting the substrate, as depicted in Figure 13, will be carried out in terms of (i) momentum transfer based on the Navier-Stokes equations (6) and (ii) the energy equation in cylindrical coordinates (7):

$$\begin{aligned}
 (\delta u / \delta t) + u(\delta u / \delta r) + v(\delta u / \delta y) &= -(1/\rho)(\delta p / \delta r) + g_r + \\
 & \quad \nu[(\delta^2 u / \delta r^2) + (\delta^2 u / \delta y^2) + ((1/r)(\delta u / \delta r) - (u/r^2))] \\
 (\delta v / \delta t) + u(\delta v / \delta r) + v(\delta v / \delta y) &= -(1/\rho)(\delta p / \delta y) + g_y + \\
 & \quad \nu[(\delta^2 v / \delta r^2) + (\delta^2 v / \delta y^2) + (1/r)(\delta v / \delta r)] \quad \dots (6)
 \end{aligned}$$

$$(\delta T / \delta t) = \alpha (\delta^2 T / \delta y^2) + (\delta^2 T / \delta r^2) + (1/r)(\delta T / \delta r) \quad \dots (7)$$

where,

u, v = velocities in the radial(r) and axial(y) directions, respectively;		
p = pressure	$\nu$ = viscosity	T = temperature
g = gravitational force	t = time	$\alpha$ = thermal diffusivity

The assumption of cylindrical symmetry for the splatting droplet significantly reduces the computational effort and computer resources. A finite difference method based on the marker and cell (MAC) method [12]

using a Eulerian staggered grid will be developed. Evaluating the location of the free surface boundary will be facilitated by introducing massless marker particles which move with the fluid onto the surface of the droplet. Due to the vast changes in dimensions of the droplet which flattens into a thin pancake during splatting, a method of continuously adapting the grid to make efficient use of the computational domain will be developed. Solidification of the droplet will be simulated by using a two-dimensional heat transfer model combined with the non-equilibrium Scheil equation [13].

These momentum and energy models are coupled by the temperature dependence of the physical properties. Resistance to fluid flow caused by solid or mushy metal will be treated by equating the local viscosity with temperature and fraction of solid.

### (c) Future Research

#### Short Term Objectives

Experiments similar to run 3 involving spray deposition onto flat substrates will be performed on the alloy compositions listed previously. These experiments will show which of the alloy compositions would be the most useful for a thorough study of the spray deposition process parameters. A number of refinements will be introduced for this research. A nozzle stopper mechanism with a built-in thermocouple will enable the melt to be poured at a known superheat. Several thermocouples embedded in the substrate and deposit will be interfaced with a computer to record the temperature and monitor changing heat flow conditions.

A Pitot tube will measure the velocity of the atomizing gas at various positions in the atomizing region during a "dry" run and a thermocouple placed inside the spray chamber will measure the temperature of the exhaust gas. These results will be incorporated into the computer modeling studies.

**Long Term Objectives**

An investigation of the spray forming process parameters will be carried out on the most suitable alloy system. This will provide a thorough knowledge of the atomization and deposition processes and lead to a complete understanding of the solidification and consolidation mechanisms. A high speed video camera (2,000 frames per second) will enable individual droplet deposition to be recorded.

## REFERENCES

1. Nichiporenko, O. S. and Naida, Yu. I. ; Soviet Powder Metall. Met. Ceram. (1968), 7(67), 1.
2. See, J. B. and Johnston, G. H. ; Powder Technology (1978) 21, 119.
3. Ranger, A. A and Nicholls, J. A ; AIAA Journal (1969) 7, 285.
4. Singer, A. R. E ; Light Metal Age (1974) 32 (9.10), 5.
5. Rao, P. ; "Shape and Other Properties of Gas Atomized Metal Powders" , Ph.D. Thesis (1973), Drexel Univ. , Philadelphia.
6. Naida, et. al. ; Soviet Powder Metall. Met. Ceram. (1980) 19(4), 217.
7. Kim, M. H.; "The Structure and Properties of Spray-Cast Deposits", Ph.D. Thesis (1982) , Univ. of Sheffield.
8. Clift, R. et. al. ; Bubbles, Drops and Particles, (1978) , Academic Press.
9. Lesinski, J. and Fanton, J. C.; AIChE Journal (1981) 27(3) , 358.
10. Ranz, W. E and Marshall, W. R ; Chem. Eng. Prog. (1952) 48, 173.
11. Kimura, I and Kanzawa, A ; AIAA Journal (1965), 476
12. Harlow, F.H. and Shanon, J.P; J. Appl. Phys. (1967) 38 (10), 3855.
13. Flemings, M.C; Solidification Processing (1974), McGraw-Hill, NY, 81.

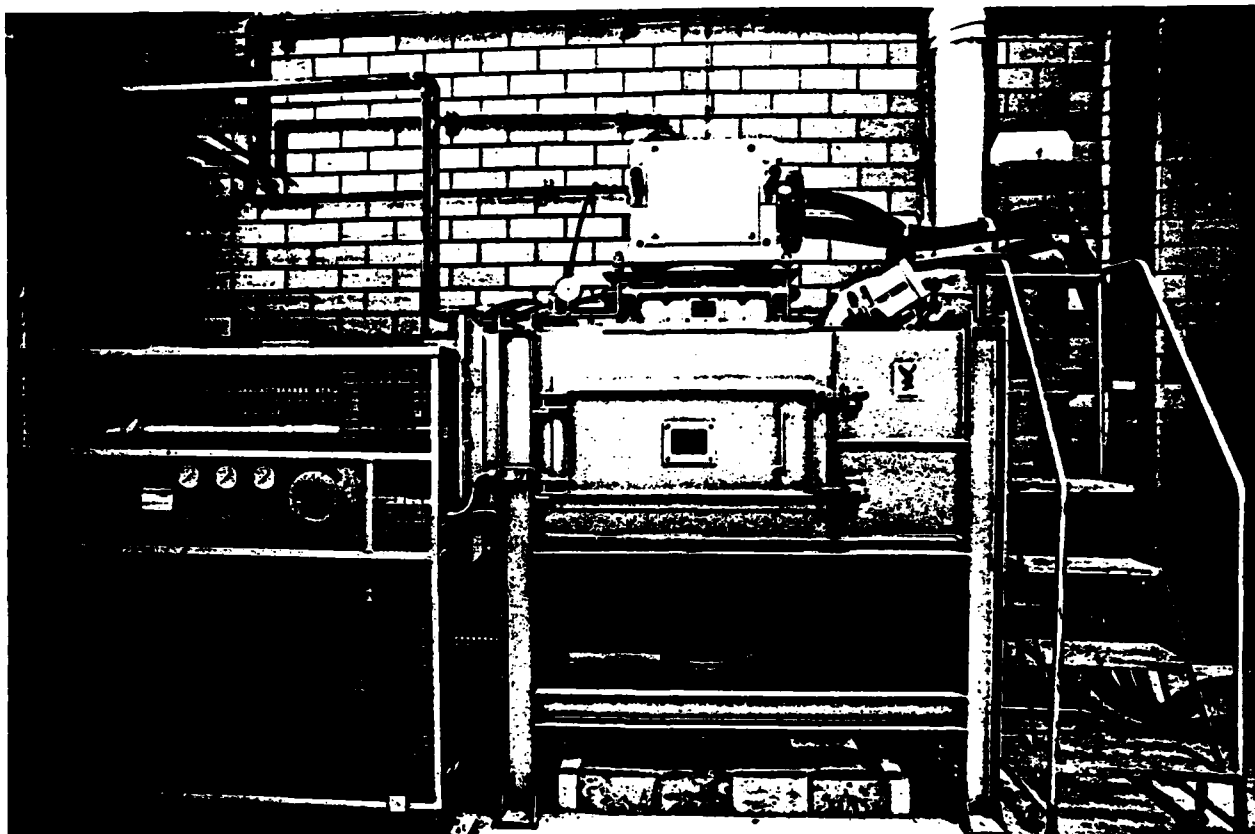


**Fig. 1: The Drexel spray forming unit.**

Accession For		
NTIS	CRA&I	<input checked="" type="checkbox"/>
DHC	TAB	<input type="checkbox"/>
Unannounced		<input type="checkbox"/>
Justification		
By		
Distribution		
Availability Codes		
Dlt	Available for Special	
A-1		

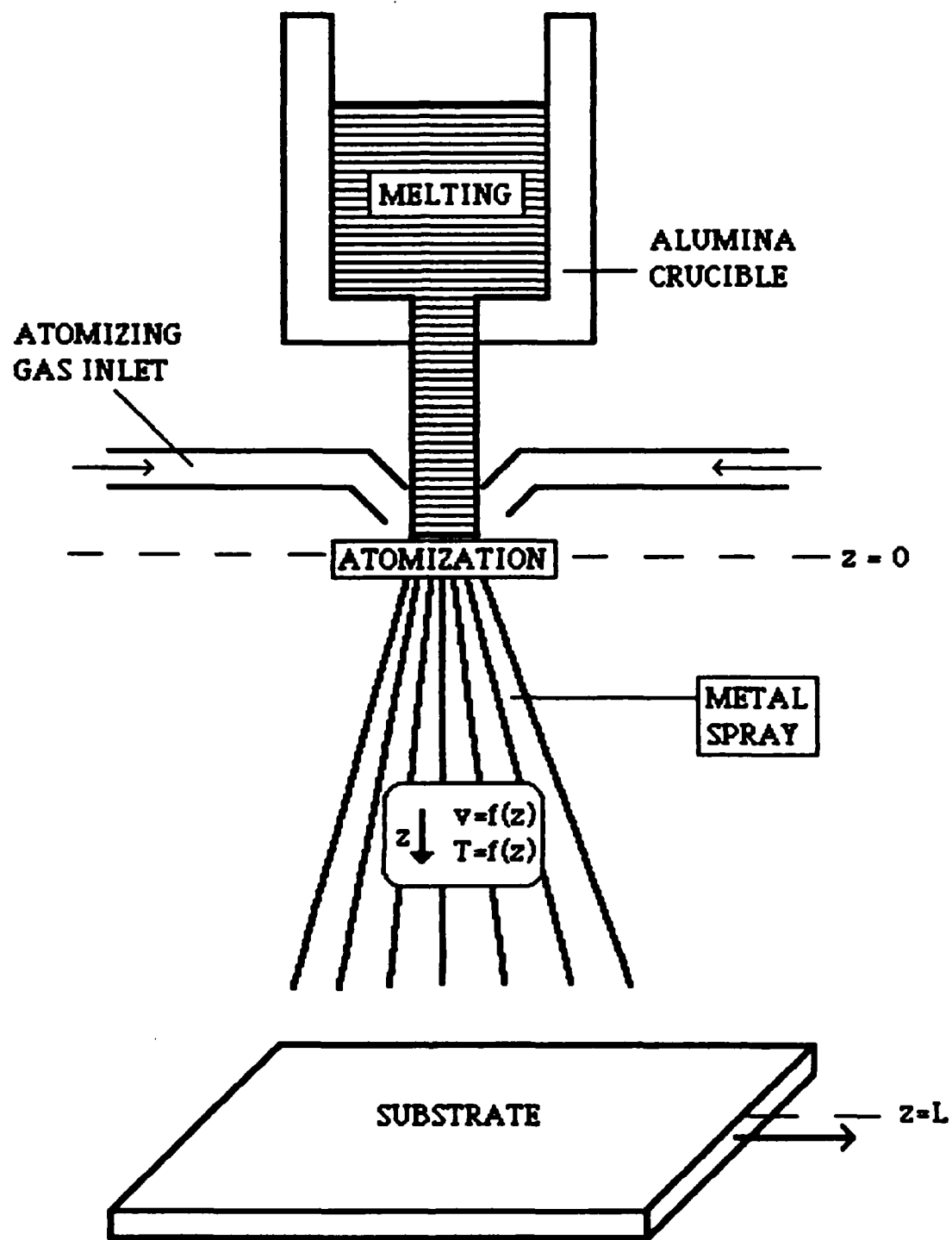
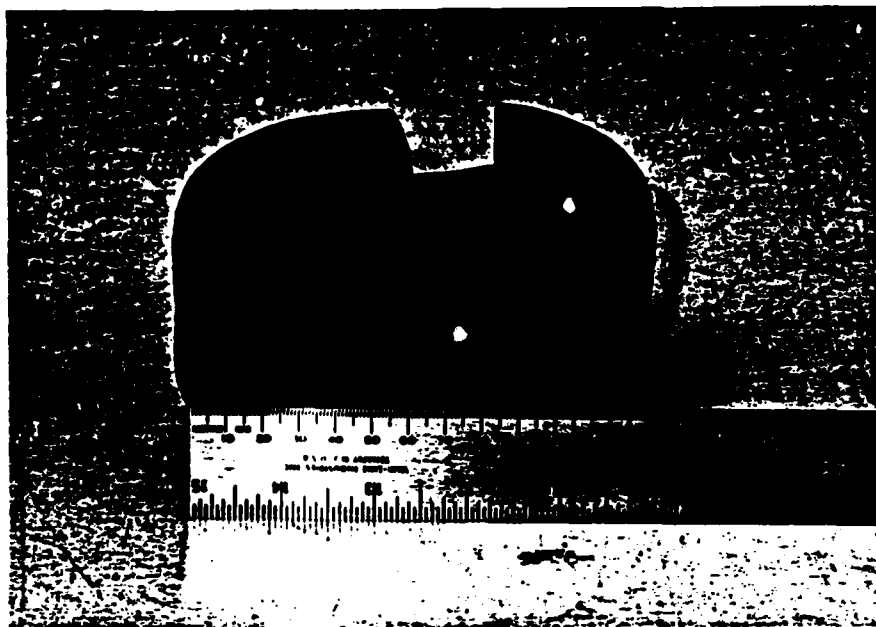
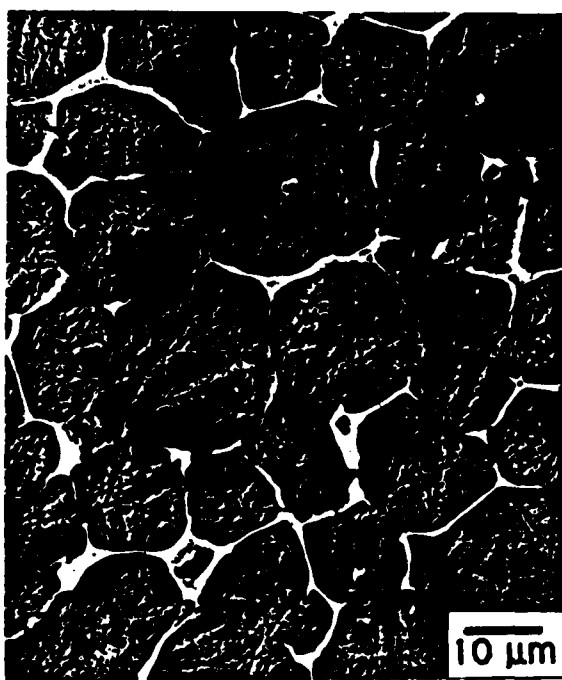


Fig. 2: Schematic illustrating the four components of the spray forming process.





**Fig. 3 : Photograph of preform from Run 2.**



**Fig. 4 : Photomicrograph from top of M2 preform.**

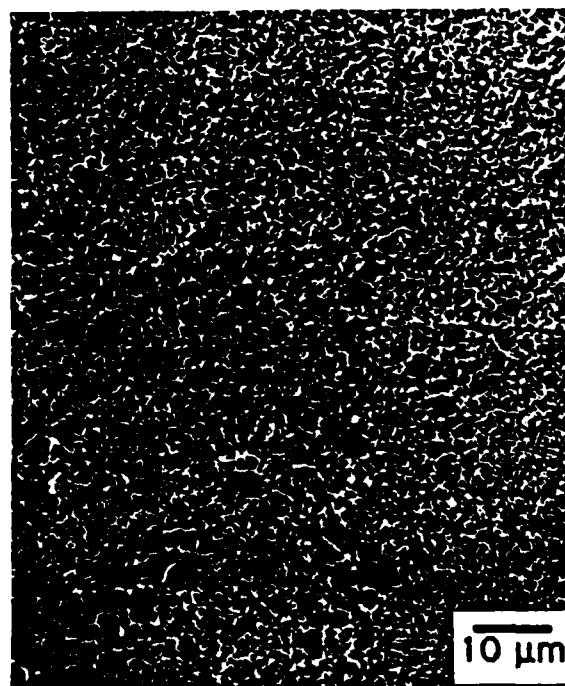


**Fig. 5 : Photomicrograph of bottom surface of preform of M2 in contact with a refractory substrate.**

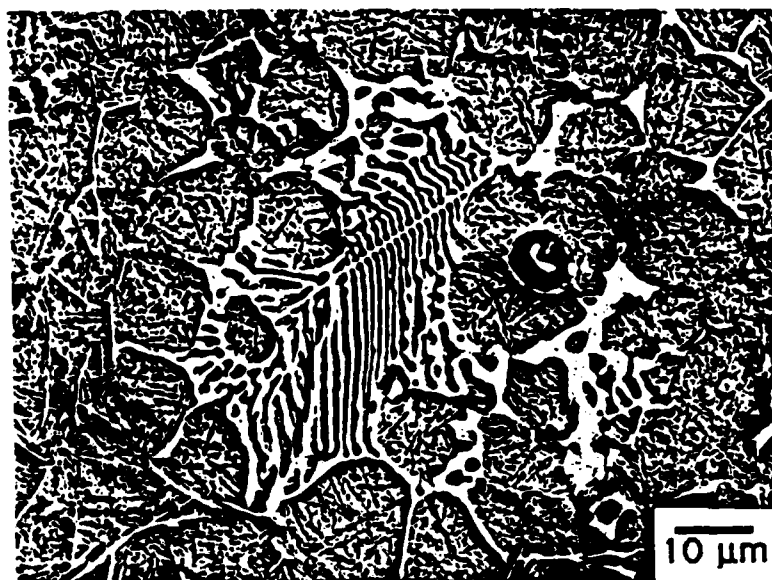


**Fig. 6 : Typical eutectic structure observed near pores and other areas of localized slow cooling.**

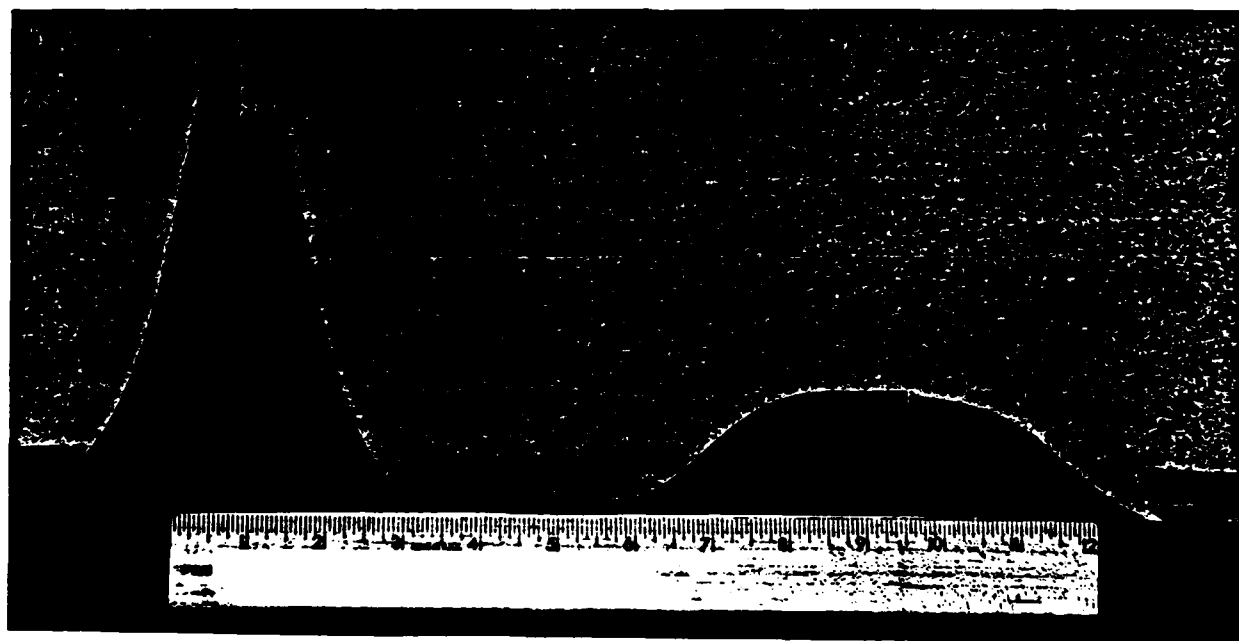
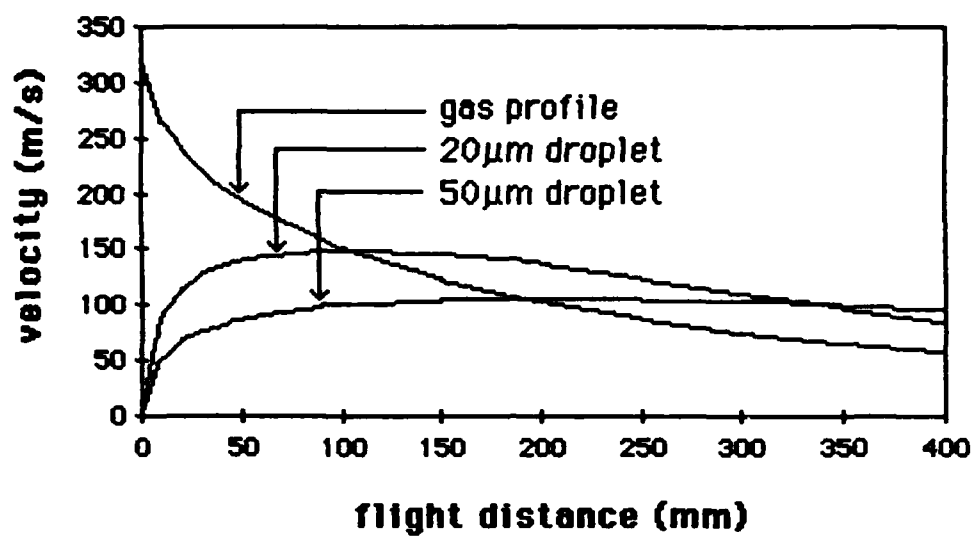
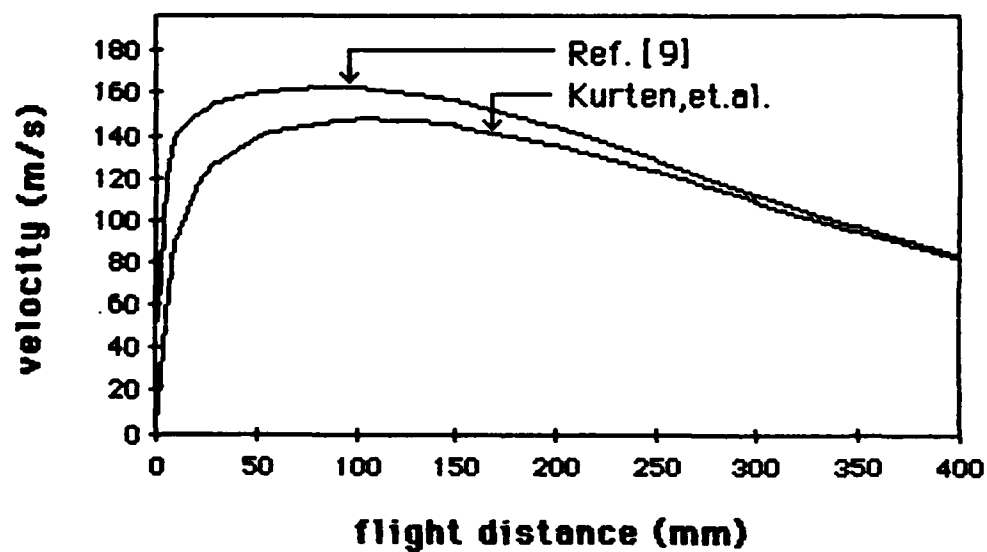


**Fig. 7 : Photograph of preform from Run 3.**

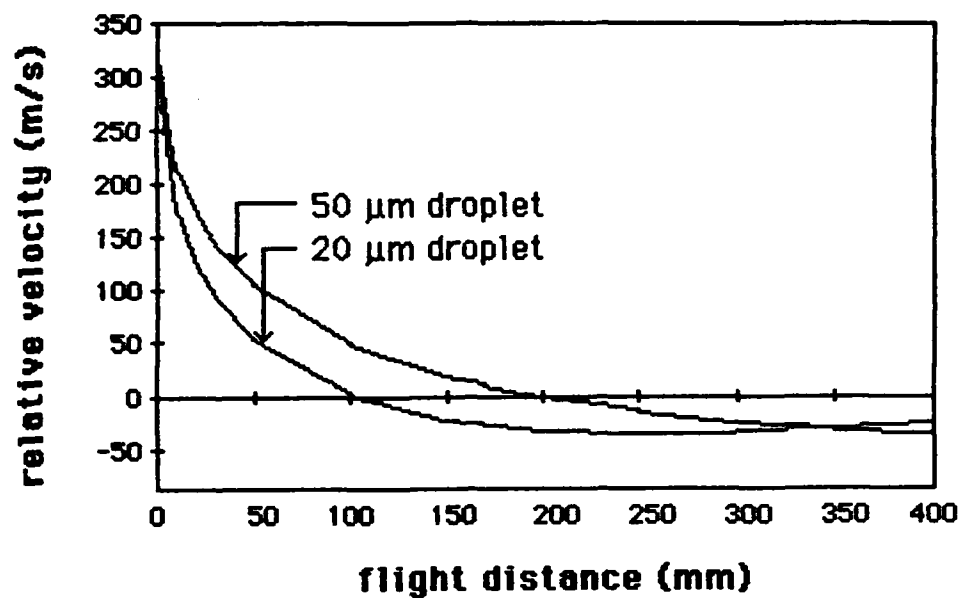


( a )

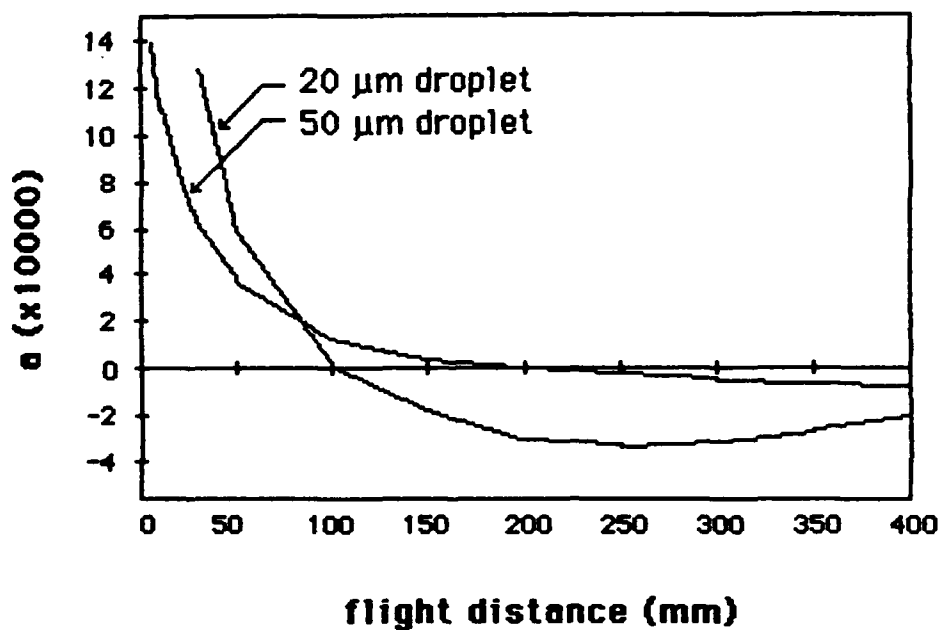


( b )

Fig. 8: Velocity vs distance plots for (a) 20μm and 50μm droplets, and (b) for 20μm droplet calculated from two measurements [8,9] of the drag coefficient.

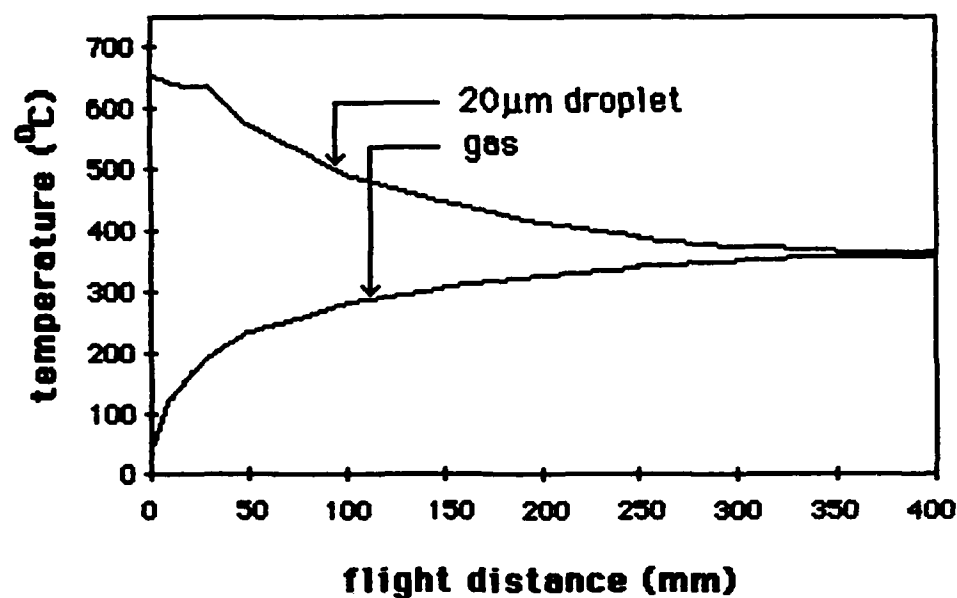


( a )

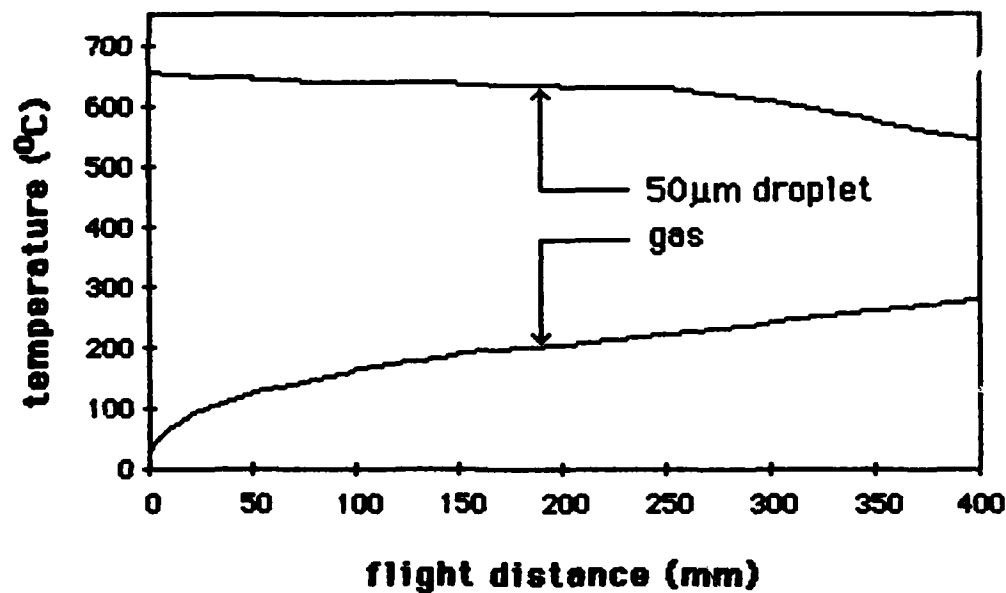


( b )

Fig. 9 : Variation of (a) the gas velocity relative to the droplet, and (b) droplet acceleration with flight distance.



(a)



(b)

Fig. 10: Temperature profiles of (a) 20µm and (b) 50µm aluminum alloy droplets with 25°C superheat.

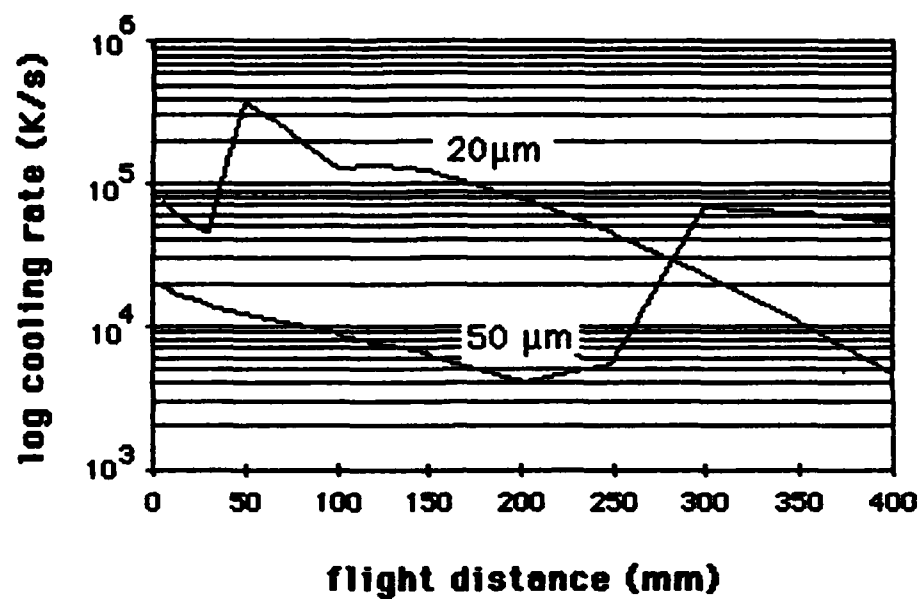
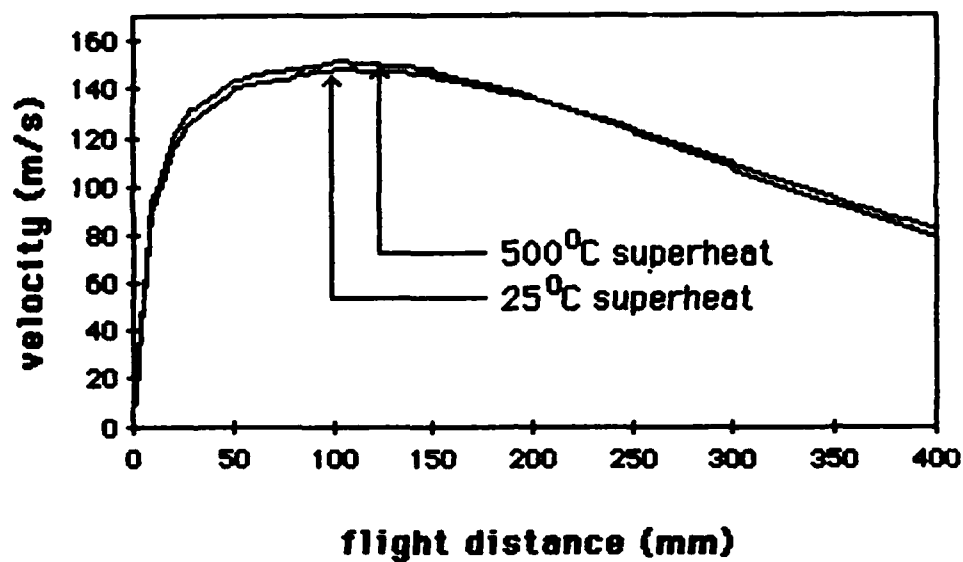
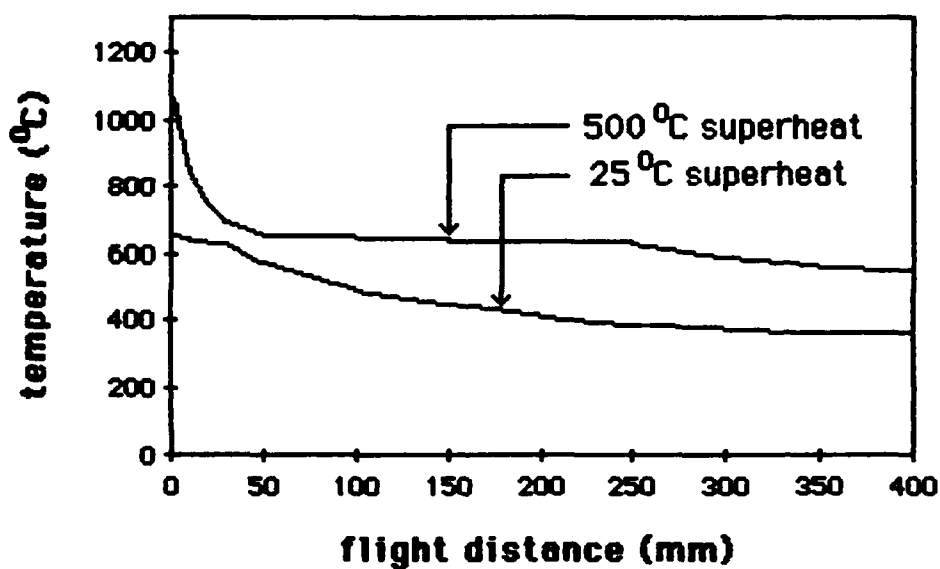


Fig. 11 : Predicted variation of cooling rate with distance for 20μm and 50μm droplets. Abrupt changes in slope correspond to start and end of mushy regions.



(a)



(b)

Fig. 12 : Effect of superheat on (a) velocity profile, and (b) temperature profile of 20 $\mu$ m droplet.

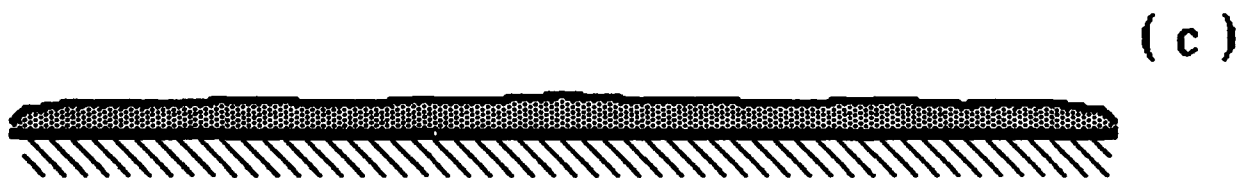
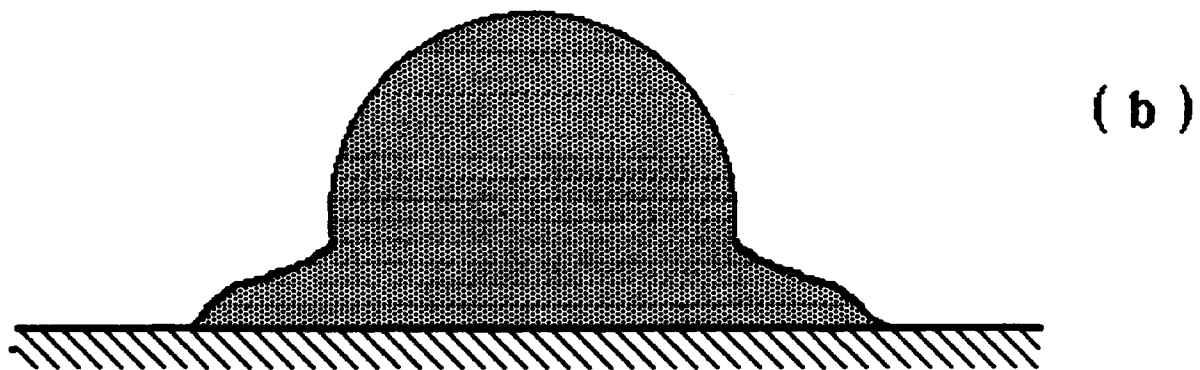
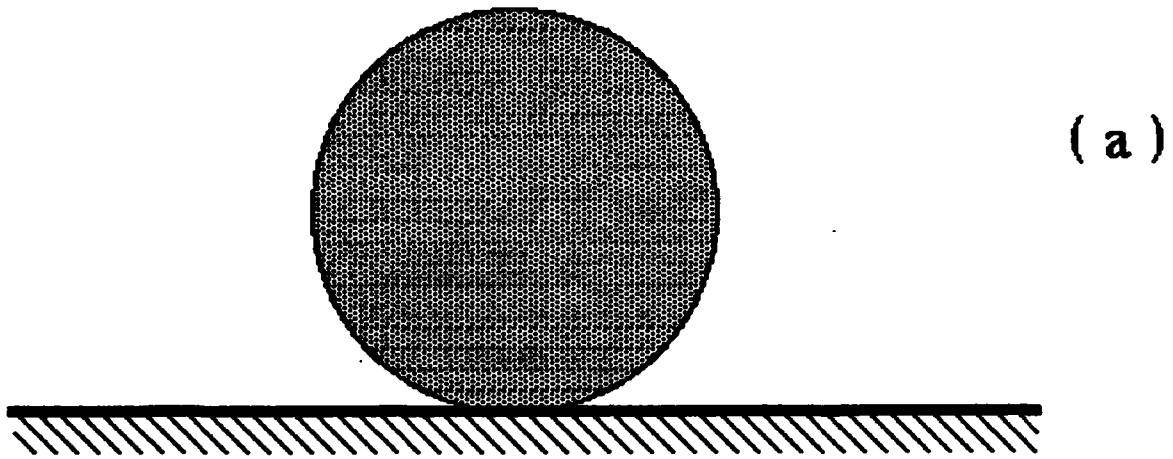


**Fig. 13: Splotting of a molten droplet on the substrate (a) initial contact, (b) partial spreading and (c) final configuration.**



**APPENDIX I : ACQUISITION, INSTALLATION, COMMISSIONING AND  
OPERATION OF THE SPRAY FORMING UNIT.**

- October 1983 : Apelian visits Osprey Metals Ltd., U.K. and the start of negotiations (Drexel funds).**
- June 1984 : Apelian visits Widmark at Sandvik, Sweden to finalize price and sale agreement (Drexel funds).**
- September 1984: Order placed with Osprey Metals Ltd., U.K. for a spray forming unit.**
- November 1984 : Lawley and Gillen visit Osprey to discuss specifications of the Drexel unit and preliminary details regarding installation.**
- January 1985 : Gentner visits Osprey to examine Drexel's unit and finalize installation plans.**
- February 1985 : Spray forming facility is shipped to Drexel University. Gillen spends three weeks at Osprey to gain a comprehensive understanding of the process.**
- April 1985 : Spray forming equipment arrives at Drexel.**
- April - June 1985 : Installation of induction generator, operating consoles and gas supply system.**
- June 1985 : Osprey engineers (Davis and Thomas) commission Drexel's spray forming facility. First run performed to produce a circular M2 tool steel preform - Osprey and Drexel personnel.**
- July 1985 : Modifications made to the gas supply system to improve uniformity of flow. Second run performed with M2 tool steel; circular preform - Drexel personnel only.**
- August 1985 : Third run - M2 spray deposited onto flat refractory and copper substrates.**

## APPENDIX II - OPERATING CONDITIONS DURING RUN 1

1. MELTING	Alloy Material :	M2 tool steel
	Charge weight :	14.1 kg / 31.1 lbs
	Nozzle diam. :	5.3 $\phi$ mm
2. ATOMIZATION	Atomizing pressure :	6.9 bar / 100 psi
3. METAL SPRAY	Spray height :	340 mm / 13.25 in.
4. SUBSTRATE	Material :	Refractory alumina
	Configuration :	120 mm diam. disc
	Rotation speed :	180 rpm
5. RUN	Preform weight :	8.82 kg (62.6% yield)
	Crucible skull :	0.06 kg (0.4%)
	Overspray :	3.97 kg (28.2%)
	Cyclone powder :	1.05 kg (7.4%)
	Run time :	40 secs
	Avg. flow rate :	0.35 kg /sec

**END**

**FILMED**

---

**1-86**

**DTIC**